Low Temperature Physics/Fizika Nizkikh Temperatur, 2013, v. 39, No. 9, pp. 1012–1020

Observation of superfluidity in two- and one-dimensions

Nobuo Wada, Mitsunori Hieda, Ryo Toda*, and Taku Matsushita

Department of Physics, Graduate School of Science, Nagoya University
Chikusa-ku, Nagoya 464-8602, Japan
E-mail: wada.nobuo@j.mbox.nagoya-u.ac.jp

Received March 4, 2013

Even though there is no long-range-ordered state of a superfluid in dimensions lower than the three-dimension (3D) such as bulk ^{4}He liquid, superfluidity has been observed for flat ^{4}He films in 2D and recently for nanotubes of ^{4}He in 1D by the torsional oscillator method. In the 2D state, in addition to the superfluid below the 2D Kosterlitz–Thouless transition temperature T_{KT}, superfluidity is also observed in a normal fluid state above T_{KT}, which depends strongly on the measurement frequency and the system size. In the 1D state of the nanotubes, superfluidity is directly observed as a frequency shift in the torsional oscillator experiment. Some calculations suggest a superfluidity of a 1D Bose fluid with a finite length, where thermal excitations of 2π-phase winding play the main role for superfluid onset of each tube. Dynamics of the 1D superfluidity is also suggested by observing the dissipation in the torsional oscillator experiment.

PACS: *67.25.bh* Thermodynamic properties;
67.25.dw Superfluidity in small clusters;
68.65.–k Low-dimensional, mesoscopic, nanoscale and other related systems: structure and nonelectronic properties.

Keywords: superfluidity, one-dimension, two-dimension, phase-winding, vortex.

1. Introduction

Since the first discovery of a superfluidity, it has been well studied for bulk ^{4}He liquid. In the famous torsional oscillator experiment by Andronikashvili [1], superfluid density was observed in the long-range-ordered state just below the λ-transition temperature. In contrast to this three-dimensional (3D) ^{4}He fluid, a mathematical proof indicates no long-range-ordering in 2D and 1D at any finite temperature [2].

However, literally 2D ^{4}He film formed on a flat solid surface was found to show a superfluid onset [3,4]. The onset was understood as the Kosterlitz–Thouless (KT) transition [5]. In the precise measurement of the superfluid density by a torsional oscillator at 10^3 Hz [4], the superfluid onset was observed at a little higher temperature than the KT temperature T_{KT}. The measurement-frequency dependence of the superfluidity in the normal state above T_{KT} was explained by a dynamic theory [6]. Accordingly, it is interesting to study up to how high a temperature the superfluidity is observed above T_{KT} at extremely high measurement frequencies [7]. In addition, dependence of the superfluid-onset temperature on a 2D system size has also been suggested in an experiment [8] and theories [9,10].

Recently, ^{4}He fluid nanotubes have been realized in 1D nanopores of FSM [11]. The nanotubes are recognized as the 1D state at low temperatures where the thermal wavelength is sufficiently longer than the tube diameter [12,13]. In this 1D state, superfluidity was confirmed by observing the frequency shift in the torsional oscillator experiment [14]. The observed 1D superfluidity shows dependence on tube size and dynamics [15]. Model calculations for some Bose fluids with finite 1D lengths suggest a superfluid onset at a finite temperature [16]. Since the onset temperature is scaled by the 1D length, the 1D superfluidity depends on the 1D system size. Dynamics of the 1D superfluidity is also suggested by a dissipation in the oscillator experiment.

In this paper, we report on system-size dependence and dynamics of superfluidity in 2D and 1D as studied for ^{4}He

* Present address: Cryogenic Research Center, The University of Tokyo, Bunkyo-ku, Tokyo 113-0032, Japan

films and nanotubes, respectively. In Sec. 2.1, measurement-frequency dependence for 2D ^{4}He film was observed up to 180 MHz [7]. From this dependence, we could estimate the core size and diffusion constant of the 2D vortex which plays the main role in the KT transition and the dynamics. System-size dependence was studied in Sec. 2.2 for ^{4}He films formed on the walls of porous glass whose pore diameter is sufficiently larger than the vortex core diameter. In Sec. 3.1, ^{4}He Bose fluids in 3D as well as 1D states were realized by adsorbing ^{4}He in nanopores with regular structures, respectively. The 3D fluid shows the characters of the 3D superfluid transition [17], while the 1D fluid shows properties of the superfluid onset obviously different from those of the 2D and 3D transitions. In Sec. 3.2, the observed system-size dependence of the 1D superfluidity is understood by the calculations for 1D Bose fluid with a finite length [16]. Dissipation observed in the torsional oscillator experiment suggests the dynamics of the superfluid in the 1D state (Sec. 3.3). Finally, Sec. 4 is devoted to a summary.

2. Dynamics and system-size dependences of 2D superfluid

2.1. Measurement-frequency dependence of 2D superfluid onset

Superfluidity in 2D has been studied for ^{4}He films adsorbed on flat solid surfaces. Superfluid onset with the universal jump of the superfluid density in the third-sound experiment [3] suggested the transition was due to the Kosterlitz–Thouless mechanism [5], where 2D superfluid vortices play a main role. Below the 2D KT transition temperature T_{KT}, all 2D vortices are bound into pairs. Above T_{KT} in the normal fluid state, there are free vortices due to the unbinding. The mean inter distance of the free vortices is almost equal to the 2D correlation length given by

$$\xi_+^{2D}(T) \approx a_0 \exp\left[2\pi / b\sqrt{T/T_{KT} - 1}\right], \qquad (1)$$

where a_0 is a vortex-core diameter, and b is a constant [5].

In a precise measurement by a torsional oscillator at 1.2 kHz, superfluid onset was observed a few percent above T_{KT}, accompanied by a dissipation peak [4]. The superfluidity in the normal state was understood by the dynamic theory [6]. The dissipation peak appears at a temperature T_p when ξ_+^{2D} equals the vortex diffusion length $r_D \simeq \sqrt{14D/\omega}$ during one period of the oscillation, where D is the diffusion constant of the 2D vortex and $\omega/2\pi$ the measurement frequency. Therefore, T_p is described as

$$\frac{T_p - T_{KT}}{T_{KT}} \simeq \frac{4\pi^2}{b^2}\left(\frac{1}{2}\ln\frac{14D}{a_0^2\omega}\right)^{-2}. \qquad (2)$$

It is interesting to see at how high a temperature the superfluidity is observed at extremely high measurement frequencies up to an ultimate frequency $(1/2\pi)14D/a_0^2$, above which Eq. (2) breaks down.

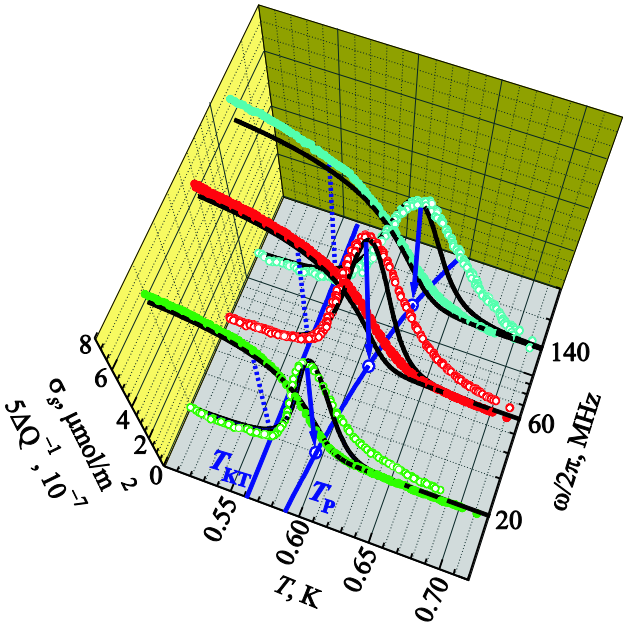

Fig. 1. (Color online) Superfluid density σ_s and dissipation ΔQ^{-1} for 2D ^{4}He film adsorbed on flat Au substrate with the KT transition temperature $T_{KT} = 0.561$ K, measured at the frequencies $\omega/2\pi = 20, 60, 140$ MHz, respectively. The superfluid-onset temperature increases with $\omega/2\pi$, and is about 20 % higher than T_{KT} for $\omega/2\pi = 140$ MHz. The peak temperature T_p of ΔQ^{-1} was fitted with Eq. (2) by using the vortex parameters $D = \hbar/m$ and a_0 the thermal de Broglie wavelength at T_{KT}.

Dynamics of the 2D superfluid was studied at extremely high-frequency measurement up to 180 MHz by a quartz-crystal microbalance [7]. Figure 1 shows the frequency dependence of observed superfluid density σ_s and dissipation ΔQ^{-1} for a ^{4}He film formed on a flat Au plate. At 140 MHz, the superfluid onset is observed about 20 % farther above $T_{KT} = 0.561$ K. The observed σ_s and ΔQ^{-1} are both well reproduced as shown by the solid curves calculated using the dynamic theory [7]. The frequency dependence of the dissipation peak temperature T_p is fitted by Eq. (2) as shown by a blue solid curve, from which the vortex parameter D/a_0^2 is obtained as shown by closed circles in Fig. 2(a). Even when the substrate is changed from bare Au to a H_2-preplating one whose adsorption potential is obviously different, D/a_0^2 has the same value for T_{KT}, as shown by squares [18]. This suggests that the diffusion constant D has the magnitude $\hbar/m$ of the quantum limit for both substrates. Thus, the vortex core diameter a_0 was estimated as shown in Fig. 2(b). It is the same magnitude as the thermal de Broglie wavelength $\lambda_{T_{KT}} = h/\sqrt{3mk_BT_{KT}}$ shown by the solid curve.

In the high-frequency measurement up to 180 MHz close to the ultimate frequency $(1/2\pi)14D/a_0^2$ for Eq. (2), dynamics of the 2D superfluidity was studied at the lowest

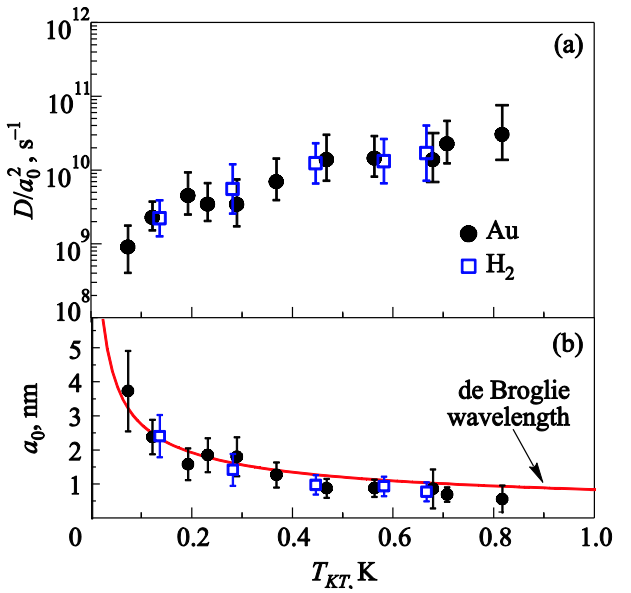

Fig. 2. (Color online) (a) 2D vortex parameter D/a_0^2 as a function of ^{4}He film thickness with T_{KT} adsorbed on flat Au (●) and H_2 preplated (□) substrates, respectively. The same magnitude of D/a_0^2 suggests the quantum limit $\hbar/m$ of the vortex diffusion constant D. (b) 2D vortex core diameter a_0 that is the same magnitude as the thermal de Broglie wavelength at T_{KT}.

temperature 70 mK. A new phase of the 2D dynamics is expected for ^{4}He films with T_{KT} below about 30 mK, where Eq. (2) will be broken down due to $\omega/2\pi \lesssim (1/2\pi)14D/a_0^2$. Another phase is also expected in a rotating condition where there are some excess vortices due to the rotation.

2.2. System-size dependence

When the bulk ^{4}He liquid was confined in a finite space with a characteristic size ℓ, the 3D superfluid-onset temperature $T_{\rm onset}^{3D}$ was observed to become a little lower than the λ-transition temperature T_λ. The difference was described by a power law as $(T_\lambda - T_{\rm onset}^{3D}) \propto \ell^{-\nu}$, when ℓ is between 2 and 10^3 nm [19]. This size dependence can be understood as the onset at $T_{\rm onset}^{3D}$ occurring when the correlation length ξ_-^{3D} of the 3D bulk superfluid becomes ℓ.

System-size dependence of the KT transition mechanism was studied for ^{4}He films formed on the pore walls of porous glass shown schematically in Fig. 3(a) [8]. The pore diameters d are greater than 5 nm which is sufficiently larger than the 2D vortex core diameter a_0 (Fig. 2(b)). The film can be regarded as being 2D only on a smaller scale than $\pi d/2$. Dependence of the superfluid-onset temperature $T_{\rm onset}$ on the pore diameter d was observed as shown in Fig. 3(b), where the onset was measured at coverages with $T_{\rm onset}$ between 0.1 and 0.7 K. $T_{\rm onset}$ for d = 290 nm was estimated to be $1.026T_{KT}$ by a theoretical fitting described in the following [8]. $T_{\rm onset}$ is always higher than T_{KT}, and it increases with decreasing d.

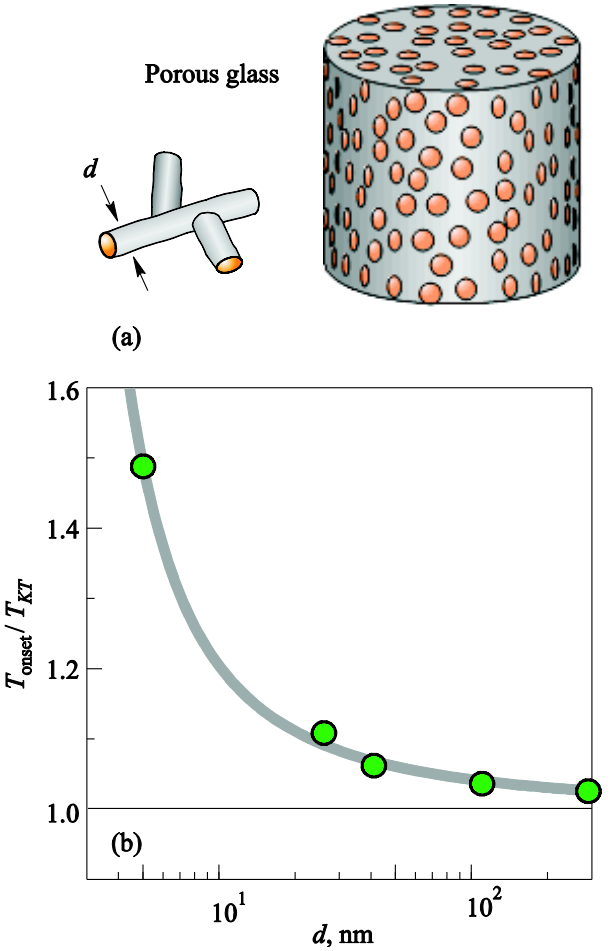

Fig. 3. (Color online) (a) Schematic view of porous glass. Pores with diameter d are randomly connected in 3D. Superfluid onset was measured for ^{4}He films adsorbed on the walls of the pores. (b) Superfluid-onset temperature $T_{\rm onset}$ relative to the 2D KT temperature T_{KT} as a function of pore diameter d. $T_{\rm onset}$ is higher than T_{KT}, and increases with decreasing d (see the text).

In the KT transition mechanism, the vortex pairing and free vortices produced by unbinding play main roles for the superfluidity [5]. The vortex pair interaction energy with intra-pair distance r in 2D is calculated to be

$$U(r) = \frac{\sigma_s^0}{2\pi}\left(\frac{h}{m}\right)^2 \ln\frac{r}{a_0}, \qquad (3)$$

where σ_s^0 is a bare superfluid density. This logarithmic dependence determines the KT transition temperature T_{KT} for sufficiently large 2D films. In the porous glasses, the logarithmic dependence remains only for the small pairs with $r \lessapprox \pi d/2$. For the pairs larger than $\pi d/2$ shown in Fig. 4(a), the superfluid flows along a "string" with the velocity $v_s = (h/m)/(\pi d)$ [9,10]. Thus, the kinetic energy of the superflow increases in proportion to the length r of the "string", and the pair potential for $r > \pi d/2$ is given as

$$U(r) = \frac{\sigma_s^0}{2\pi}\left(\frac{h}{m}\right)^2 \frac{r}{d}, \qquad (4)$$

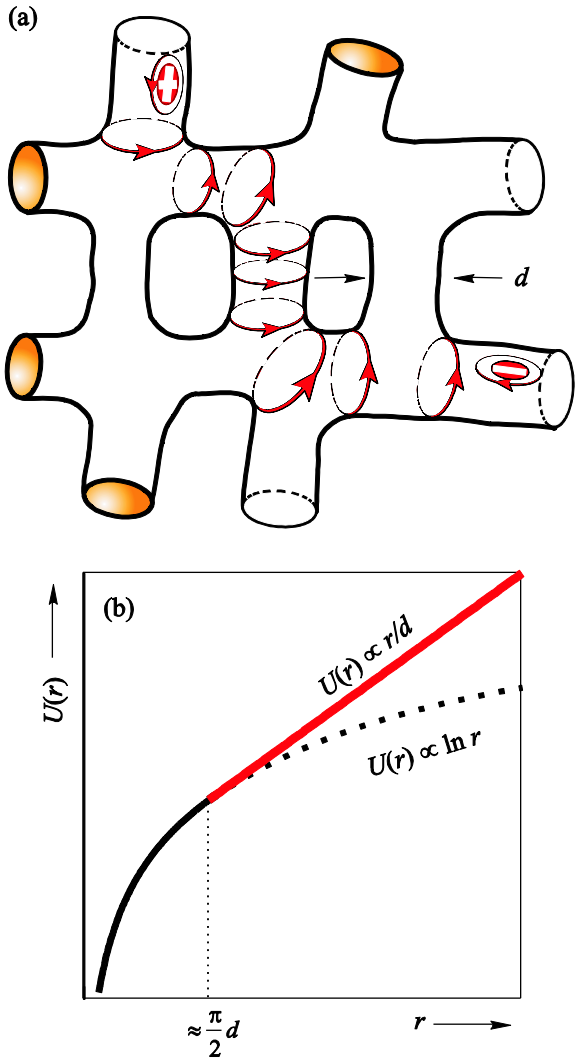

Fig. 4. (Color online) (a) A vortex pair larger than $\pi d/2$ in porous glass. Around the "string" with length r, there is a superfluid flow of $v_s = (h/m)/(\pi d)$. The flow energy is proportional to r/d as given in Eq. (4). (b) Vortex pair potential $U(r)$. $U(r)$ of a small pair with $r \lessapprox \pi d/2$ is the same ln r-dependence as that of the flat film given in Eq. (3). $U(r)$ of larger pair (Eq. (4)) has the linear dependence which induces a strong force confining vortices to a pair.

as shown in Fig. 4(b). The vortices are bound into a pair for $r \lessapprox \pi d/2$ by much larger constant force of $-(dU/dr) \propto 1/d$ than $-(dU/dr) \propto 1/r$ of the logarithmic potential (Eq. (3)). The strong confinement force causes the onset temperature $T_{\rm onset}$ in the porous glass to become higher than T_{KT}. $T_{\rm onset}$ was estimated when $\xi_+^{2D}(T)$ of Eq. (1) equals $\pi d/2$. This well explains the pore size d dependence of the onset temperature shown in Fig. 3(b) [8].

In the case of 2D ^{4}He films, both dependences on the measurement frequency and the system size show that the superfluid-onset temperature becomes higher than the KT temperature.

3. Superfluidity in 1D state with finite length

3.1. Observation of superfluidity of ^{4}He nanotubes

Since 1993, nanoporous materials have been synthesized which have regular structures and many kinds of dimensional pore connection (topology) and diameters [11,20]. We have been studying new kinds of superfluid transitions (onsets) for ^{4}He adsorbed in these nanopores. We first had to know how ^{4}He atoms were adsorbed in the nanopores. Adsorption energy of the ^{4}He adatoms and evolution of a uniform layer on the nanopore walls were observed by measuring pressure isotherms for the adsorption and heat capacity [13,21].

The dependence of the superfluidity on the dimensionality was studied for ^{4}He adsorbed in 1D and 3D nanopores (upper insets in Fig. 5) [17]. Although the nanopores have different 1D and 3D pore connections (topologies), both have almost the same pore diameter (2.8 and 2.7 nm) and adsorption potential [22]. Uniform layers are formed up to about 2 atomic layers. Figures 5(a) and (b) show the heat capacity (C) and the superfluid density ($\propto \Delta f$) measured by the torsional oscillator at almost the same coverage n of ^{4}He about 1.7 atomic layers.

^{4}He films in the 3D nanopores show a sharp peak of the heat capacity at T_C (Fig. 5(b)). The superfluid-onset temperature $T_{\rm onset}$ is the same as the peak temperature T_C of the heat capacity, within the experimental uncertainty. This is one of the main properties of the 3D phase transition. In the torsional oscillator experiment, dissipation was not observed except for that by the coupling with standing waves of the third sound. No observation of the dissipation accompanied by the superfluid onset is likely to be a property of the 3D transition of the 3D ^{4}He films, or of the bulk superfluid transition.

In case of the 1D nanopores (Fig. 5(a)), the heat capacity shows a hump at T_C instead of a sharp peak. Furthermore, the superfluid onset of the ^{4}He nanotubes is observed at $T_{\rm onset}$ which is far below the heat capacity anomaly at T_C. At the low temperatures, the thermal phonon wavelength is calculated to be longer than the ^{4}He fluid tube diameter [13], which is a definition of the 1D state. Thus, the superfluidity was observed in the 1D state by the torsional oscillator.

The 1D superfluidity was observed above the ^{4}He coverage about 24 μmol/m^2 (1.4 atomic layers) in the 1D nanopores 2.8 nm in diameter, as shown in Figs. 6(a) and (b). Below the onset temperature, Δf increased more slowly than the steep increase of the 2D KT transition. The observed Δf is mainly that of the ^{4}He nanotubes, as described in the following. Below the onset temperature, ΔQ^{-1} shows a characteristic large peak (Fig. 6(b)). The large peak temperature T_X is obviously lower than the onset temperature and T_{KT} of a tiny peak which is the dissipation peak due to the 2D KT transition of the ^{4}He films covering the grain surfaces. This large peak cannot be ex-

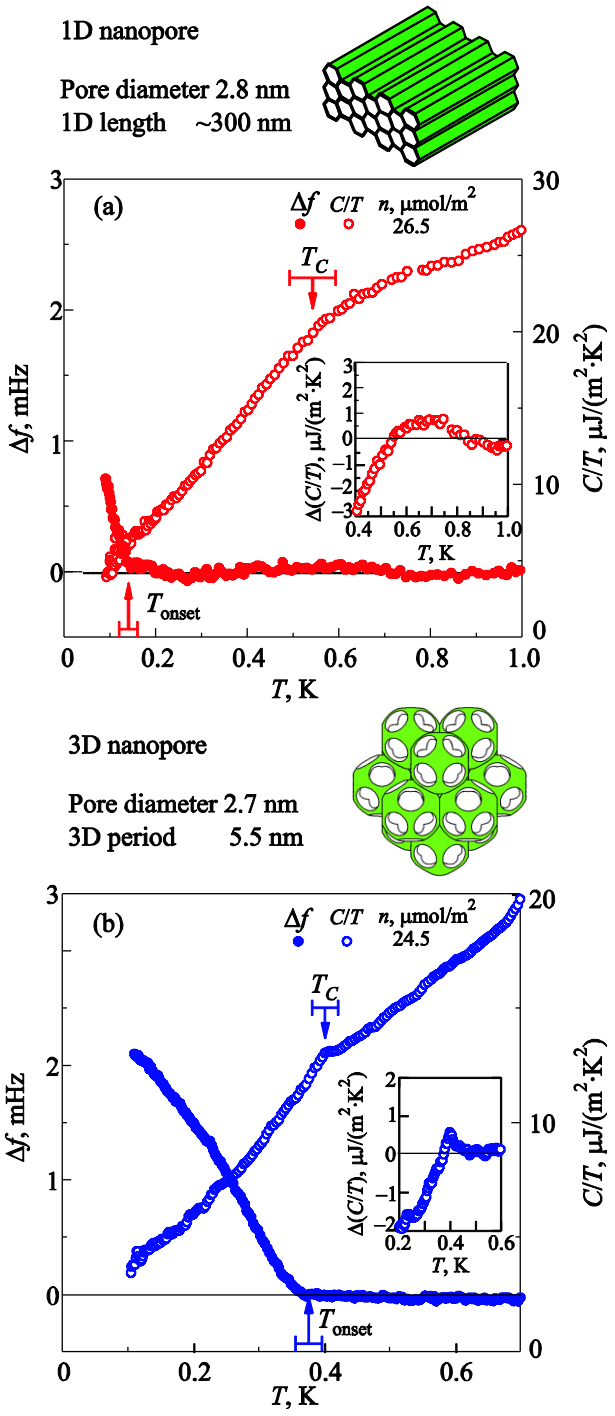

Fig. 5. (Color online) Superfluid density ($\propto \Delta f$) and heat capacity C of ^{4}He adsorbed in 1D nanopores of FSM (a) and in 3D nanopores of HMM-2 (b), respectively. Obvious differences are due to the dimensionality of the film connection. In the 1D nanopores, the observed superfluidity is in the 1D state where the thermal phonon wavelength is estimated to be longer than the pore diameter. In the 3D nanopores, 3D superfluid transition is suggested by the sharp heat capacity peak at the superfluid-onset temperature.

plained by the frequency and size effect for the KT mechanism described in Sec. 2, because T_X is obviously lower

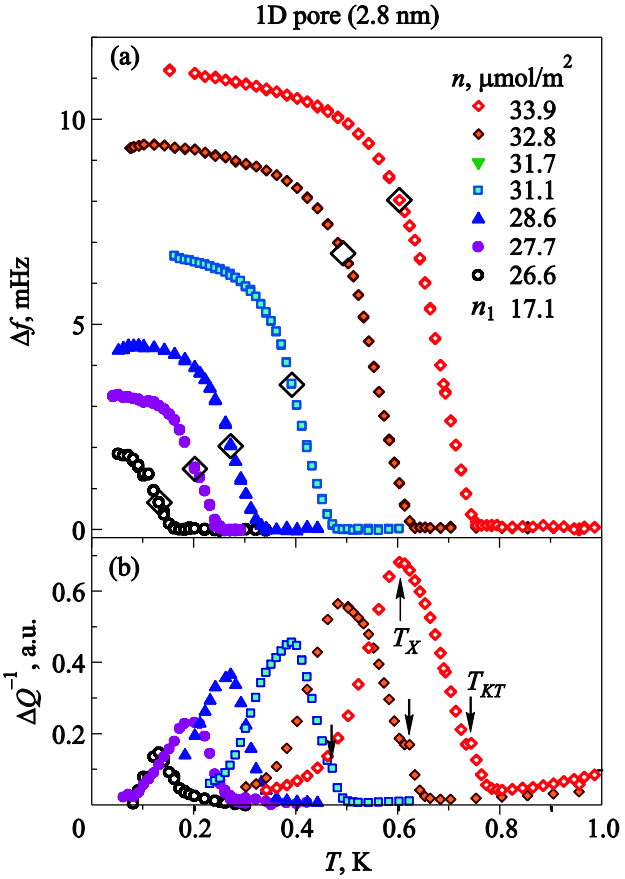

Fig. 6. (Color online) Superfluidity of ^{4}He nanotubes formed in 1D nanopores 2.8 nm in diameter as a function of coverage n observed by a torsional oscillator. n_1 is the first layer coverage. (a) Superfluid frequency shift Δf that is proportional to the superfluid density. Below the onset temperature, Δf increases more slowly than the jump-like increase of the 2D KT transition. (b) Dissipation ΔQ^{-1} which shows a dynamic property for the measurement frequency of 1.2 kHz. Very large peak at T_X below T_{KT} is accompanied by the superfluidity of the ^{4}He nanotubes.

than T_{KT}. Thus, the large dissipation peak at T_X is likely to be one character of the 1D superfluidity.

In order to observe a system-size dependence of the 1D superfluidity, superfluid shift Δf was measured for ^{4}He nanotubes formed in the 1D nanopores which have almost the same length about 300 nm but different diameters d from 1.5 to 4.7 nm [14,15]. The ^{4}He nanotubes in the fluid state are adsorbed on inert ^{4}He layers about 0.5 nm in thickness covering the nanopore walls. Therefore, the fluid tube diameter is reduced about 1 nm from the bare pore diameter d.

The pore-diameter dependence of Δf is shown in Fig. 7 for films whose onset temperatures T_{onset} are about 1 K [15,23]. They indicate Δf per unit adsorption area against the reduced temperature T/T_{onset} with solid circles. We also measured the KT transition of the films covering the FSM grain surfaces by filling the nanopores with N_2, as shown by solid curves. The difference shown by the shaded region is the superfluid shift Δf of the ^{4}He nano-

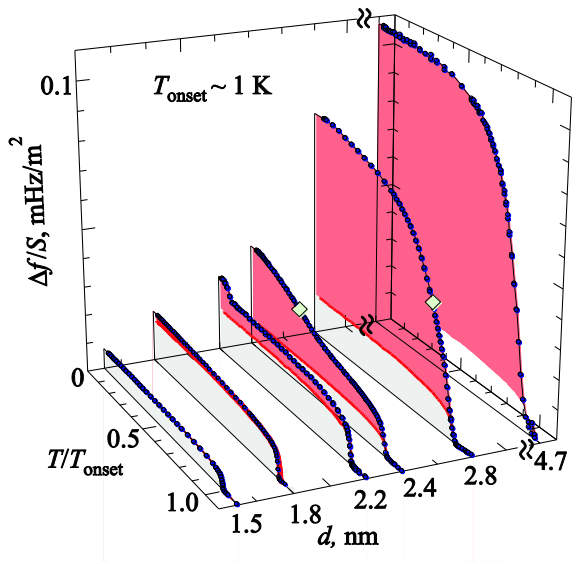

Fig. 7. (Color online) Superfluid shift $\Delta f / S$ per specific area for 1D pore diameters d from 1.5 to 4.7 nm. Temperature is normalized by the onset temperature T_{onset} about 1 K. Bottom curve is $\Delta f / S$ of the films covering grain surfaces which shows the KT transition. Dark shaded region between the solid circles and the bottom curve shows $\Delta f / S$ of the ^{4}He nanotubes. Superfluidity of the nanotubes was observed for the 1D pores of $d \geq 1.8$ nm. The large dissipation peak characteristic of the 1D superfluidity is observed at the temperature marked with ◇ for d = 2.4 and 2.8 nm.

tubes. The result indicates that Δf of the ^{4}He nanotubes was observed for the pore diameter above 1.8 nm. $\Delta f / S$ of the nanotubes in the 1.8 nm pores appears below T_{onset}, and it increases very slowly with decreasing temperature down to the lowest temperature measured. In the case of 2.4 nm pores, $\Delta f / S$ of the nanotubes increases slowly below T_{onset}, and it increases rather rapidly around $T / T_{\text{onset}} \approx 0.4$. Around the same temperature marked by ◇ ($T / T_{\text{onset}} = 0.38$) in Fig. 7, a large dissipation peak of ΔQ^{-1} was observed in addition to the tiny KT peak just below T_{onset}. We call the crossover temperature of $\Delta f / S$ as T_X which is determined to be the same as the dissipation peak temperature in the present experiment. In the case of 2.8 nm pores, the crossover temperature is determined to be $T_X / T_{\text{onset}} = 0.83$ at the dissipation peak, similar to that in Fig. 6(b). $\Delta f / S$ for the largest 4.7 nm pores steeply increases below T_{onset}, followed by the almost constant dependence. It can be understood that the full magnitude of $\Delta f / S$ of the ^{4}He nanotubes was observed below the KT temperature of ^{4}He films on the grain surfaces [24].

There have been few observations of the superfluidity in the 1D state to our knowledge, besides the present ^{4}He nanotubes. Recently, Taniguchi and Suzuki measured a superfluid by a torsional oscillator for ^{4}He liquid filling the 2.8 nm nanopores of FSM [25,26]. With increasing pressure on the ^{4}He liquid columns, they observed a quantum phase transition at about 2.1 MPa from the superfluid to a normal fluid state. The liquid has much stronger correlations than those of the ^{4}He nanotube, because of high liquid density under that pressure. The strongly correlated ^{4}He Bose liquid is expected to have a high phonon velocity, so that the fluid of the columns is in the 1D state where the phonon wavelength is larger than the column diameter. At about 1 MPa, Δf increases rather rapidly with decreasing temperature, accompanied by a large dissipation peak. They are similar to those observed for the present ^{4}He nanotubes.

3.2. Superfluidity in 1D state with finite length

In the torsional oscillator experiment for the bulk ^{4}He liquid, the frequency shift Δf correctly corresponds to the superfluid density in the second order transition. Thus, Δf is observed just below the lambda temperature with the universal critical index. In the 2D KT transition, however, the superfluid density is observed as the shift Δf is equal to the bare superfluid density σ_s^0 only at sufficiently low temperatures. With increasing temperature, Δf is observed to be smaller than the bare superfluid density by the shielding effect of the vortex pairs, and it disappears above T_{KT} with a universal jump, in terms of the static KT theory [5]. Alternatively, the observable superfluid density (Δf) was calculated by the Monte Carlo simulation [27] for a 2D XY ferromagnetic spin lattice [28], where calculated helicity modulus Υ [29] is assumed to be equal to Δf.

Yamashita and Hirashima [16] have calculated the helicity modulus Υ for spin lattices shown in Fig. 8(a) which are modeled on the ^{4}He nanotubes formed in FSM. Υ of the 2D KT transition was calculated for the 80×80 isotropic lattice, as shown in Fig. 8(b). Υ steeply changes at the KT temperature $k_B T / J \simeq 1$, corresponding to the universal jump. This calculation for the isotropic 2D lattice shows Υ of the film covering the grain surface. Corresponding to the ^{4}He nanotubes with length L and circle w, $39\times((w+1)\times 7+2)$ lattice is replaced with seven stripes, each of which has a length of 40 sites and width of w sites (Fig. 8(a)). To learn the pore-diameter dependence, Υ was calculated along the x direction by changing w from 1 to 5 lattices, as shown in Fig. 8(b). The lower curve for each w shows the KT transition of the part of the 2D spin lattice. The difference (dark shaded region) between the two curves is Υ of the stripes corresponding to the nanotubes. Υ of the stripes appears below the 2D KT temperature $\approx J / k_B$. Here, we define a crossover temperature T^* where Υ of the stripes becomes half of that at $T = 0$. Since $w \propto d$, the dependence of T^* on w qualitatively agrees with the pore-diameter dependence of T_X shown in Fig. 7. Thus, the crossover temperature T^* of the stripes is likely to correspond to T_X of the nanotubes in the experiment.

To focus on the superfluidity in 1D, Υ was calculated for stripes of length L and width w with the same aspect

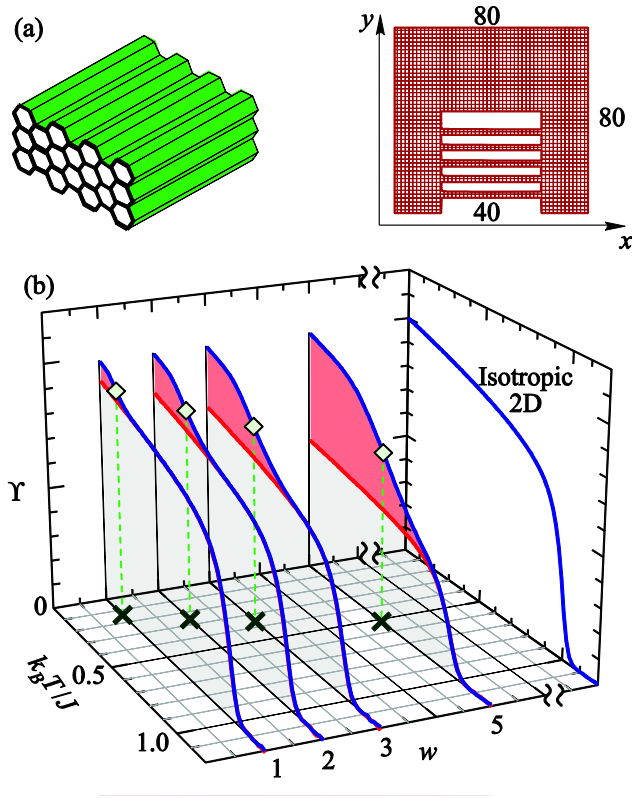

Fig. 8. (Color online) (a) Spin lattice modeled on ^{4}He nanotubes and films on FSM grain surface. Each long lattice corresponding to a nanotube has length L of 40 sites and w width sites. w is changed from 5 to 1. (b) Monte Carlo calculation of helicity modulus Υ along x-axis for the XY spin lattice. Below the 2D KT temperature $(k_BT/J \simeq 1)$, Υ of $L\times w$ long spin lattices appears as shown by the dark shaded region. Lattice width w dependence of T^* ($\diamond$) of the long spin lattices is likely to agree qualitatively with the pore size d dependence of T_X in Fig. 7.

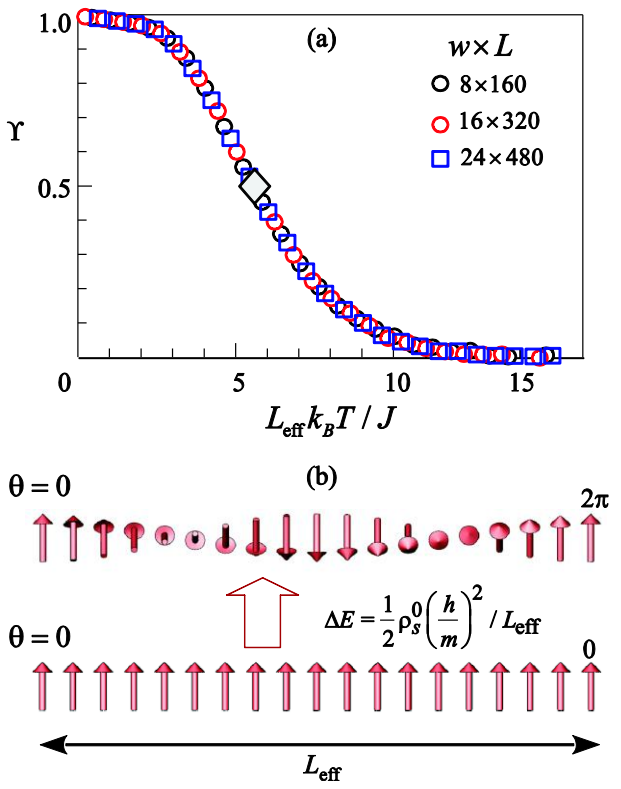

Fig. 9. (Color online) (a) Helicity modulus Υ of 1D spin lattices with the same effective 1D length $L_{\rm eff} = 20$ which is an aspect ratio of the length L divided by the width w. Temperature dependence is scaled by $TL_{\rm eff}$. Υ is measurable (onset) at $k_BTL_{\rm eff}/J \approx 10$. 1D crossover temperature T^* is defined as half of the full magnitude of $\Upsilon = 1$, shown by $\diamond$. (b) 2π-phase winding in 1D with length $L_{\rm eff}$. Since the excitation energy ΔE is proportional to $1/L_{\rm eff}$, superfluid onset and the crossover temperature (T^*) for 1D system with finite length changes as $1/L_{\rm eff}$ (see the text).

ratio $L/w = 20$ [30]. Using the effective 1D length $L_{\rm eff}$ as the aspect ratio, Υ are collapsed into the same curve for the reduced temperature $k_BTL_{\rm eff}/J$ as shown in Fig. 9(a), where J/k_B is the same as the KT temperature in the isotropic 2D lattice. The calculated Υ gradually increases with decreasing temperature. Υ is measurable below $k_BTL_{\rm eff}/J \simeq 10$, and it becomes half of the full magnitude ($\Upsilon = 1$) at $k_BTL_{\rm eff}/J = 5.5$ which is equal to T^* ($\diamond$) in Fig. 8(b). The 1D superfluid onset and the crossover temperature T^* decrease with increase in the effective 1D length $L_{\rm eff}$, which explains qualitatively the pore-diameter d dependence of T_X in Fig. 7.

The characteristic dependence of the 1D superfluidity on $L_{\rm eff}$ can be understood by considering the thermal excitation of a 2π-phase winding as shown in Fig. 9(b) [16,31–33]. In the XY spin model, the excitation energy is calculated to be

$$\Delta E = \frac{1}{2} J(2\pi)^2 / L_{\rm eff}. \qquad (5)$$

This is equal to $\Delta E = (1/2)\rho_s^0(h/m)^2/L_{\rm eff}$ for the 1D superfluid, where ρ_s^0 is the bare 1D superfluid density. Probability for thermally exciting the 2π-phase winding in a 1D lattice is given as $P \propto \exp[-\Delta E/k_BT]$. At sufficiently low temperatures, $P \simeq 0$, and then full magnitude of $\Upsilon = 1$ is observed even in the 1D state. With increasing temperature, Υ decreases in proportion to P due to the excitations of 2π-phase windings. As a result, the crossover temperature T^* is proportional to $1/L_{\rm eff}$. Almost the same size dependence of the superfluid density (Υ) was calculated for the Tomonaga–Lattinger liquid [34] and a 1D Bose–Hubbard system [35], by adopting some proper correspondences for $L_{\rm eff}$. Thus, this size effect is one of the main properties of the 1D superfluidity.

3.3. Dynamics of superfluidity in 1D state

In the measurement by the torsional oscillator at 10^3 Hz, the 3D transition of the bulk ^{4}He liquid is observed by the onset of the frequency shift Δf, where the dissipation is not observed. Even for the ^{4}He films, in the 3D na-

nopores of HMM-2, the dissipation was not observed at the 3D transition of Fig. 5(b) [17]. For 2D ^{4}He films, both Δf and the dissipation ΔQ^{-1} are observed in the KT transition (Sec. 2.1). These are quantitatively well explained by the dynamic theory, and have the Kramers–Kronig relation.

In the ^{4}He-fluid nanotubes, the large dissipation ΔQ^{-1} was observed by the torsional oscillator (Fig. 6(b)). Maximum of ΔQ^{-1} appears at the crossover temperature T_X where the temperature dependence of Δf becomes steep as shown in Figs. 7 and 8(b). Similar maximum of ΔQ^{-1} was also observed in the ^{4}He liquid column under the pressure [25,26]. The dissipation is suggested to be due to a phase slip in the nanotube, which is shown in Fig. 9(b) as an excitation of the 2π-phase winding. Relaxation probabilities of the phase slip at finite temperature were studied for XY spin models [36]. Dynamic property of the 1D system under the ac superflow was calculated for the Tomonaga–Lattinger model [37] and a 1D Bose–Hubbard model [38]. Their calculations suggest that the superfluidity is observed even for a long 1D system at a finite measurement frequency. The observed superfluid density and dissipation will depend obviously on the measurement frequency.

4. Summary

Even though there is no long-range-ordered superfluid state in the dimensions lower than 3D, superfluidity has been observed by the frequency shift Δf of the torsional oscillator in 2D and 1D.

Characteristic dynamics of the 2D KT transition was observed up to extremely high measurement frequencies, which provided detailed knowledge about 2D superfluid vortices. System-size (topology) dependence of the KT mechanism was observed for films in porous glass. The strong confinement force for a vortex pair larger than the pore diameter causes a superfluid-onset temperature higher than the 2D KT temperature.

Superfluidity in the 1D state has been recently observed for ^{4}He nanotubes formed in 1D nanopores. The pore-diameter dependence of the 1D superfluid was understood as the dependence of the 1D superfluid on the effective 1D length. Thermal excitations of the 2π-phase winding play a main role in the superfluid onset of the 1D ^{4}He fluid with finite length. Dynamics due to the phase slip was also suggested by the dissipation peak observed around the 1D crossover temperature. These superfluid properties can be observed in superconductors and atomic gases in the 1D state.

Acknowledgment

The authors thank K. Yamashita and D.S. Hirashima for variable discussions and comments about the superfluidity in one-dimension; they also supplied the calculations shown in Figs. 8(b) and 9(a).

1. E.L. Andronikashvili, *Zh. Eksp. Teor. Fiz.* **18**, 424 (1948).
2. P.C. Hohenberg, *Phys. Rev.* **158**, 383 (1967).
3. Isadore Rudnick, *Phys. Rev. Lett.* **40**, 1454 (1978).
4. D.J. Bishop and J.D. Reppy, *Phys. Rev. Lett.* **40**, 1727 (1978).
5. J.M. Kosterlitz and D.J. Thouless, *J. Phys. C* **6**, 1181 (1973).
6. Vinay Ambegaokar, B.I. Halperin, David R. Nelson, and Eric D. Siggia, *Phys. Rev. Lett.* **40**, 783 (1978).
7. Mitsunori Hieda, Kenji Matsuda, Tsuyoshi Kato, Taku Matsushita, and Nobuo Wada, *J. Phys. Soc. Jpn.* **78**, 033604 (2009).
8. K. Shirahama, M. Kubota, S. Ogawa, N. Wada, and T. Watanabe, *Phys. Rev. Lett.* **64**, 1541 (1990).
9. T. Minoguchi and Y. Nagaoka, *Prog. Theor. Phys.* **80**, 397 (1988).
10. J. Machta and R.A. Guyer, *Phys. Rev. Lett.* **60**, 2054 (1988).
11. S. Inagaki, Y. Fukushima, and K. Kuroda, *J. Chem. Soc.-Chem. Commun*. **08**, 680 (1993).
12. Nobuo Wada, Junko Taniguchi, Hiroki Ikegami, Shinji Inagaki, and Yoshiaki Fukushima, *Phys. Rev. Lett.* **86**, 4322 (2001).
13. Nobuo Wada and Milton W. Cole, *J. Phys. Soc. Jpn.* **77**, 111012 (2008).
14. Hiroki Ikegami, Yoji Yamato, Tomohisa Okuno, Junko Taniguchi, Nobuo Wada, Shinji Inagaki, and Yoshiaki Fukushima, *Phys. Rev. B* **76**, 144503 (2007).
15. N. Wada, Y. Minato, T. Matsushita, and M. Hieda, *J. Low Temp. Phys.* **162**, 549 (2011).
16. K. Yamashita and D.S. Hirashima, *Phys. Rev. B* **79**, 014501 (2009).
17. Ryo Toda, Mitsunori Hieda, Taku Matsushita, Nobuo Wada, Junko Taniguchi, Hiroki Ikegami, Shinji Inagaki, and Yoshiaki Fukushima, *Phys. Rev. Lett.* **99**, 255301 (2007).
18. Takuya Oda, Mitsunori Hieda, Ryo Toda, Taku Matsushita, and Nobuo Wada, *J. Low Temp. Phys.* **158**, 262 (2010).
19. N. Wada, A. Inoue, H. Yano, and K. Torii, *Phys. Rev. B* **52** (1995) **1167**, and the references therein.
20. S. Inagaki, S. Guan, Y. Fukushima, T. Ohsuna, and O. Terasaki, *J. Am. Chem. Soc*. **121**, 9611 (1999).
21. Nobuo Wada, Taku Matsushita, Mitsunori Hieda, and Ryo Toda, *J. Low Temp. Phys.* **157**, 324 (2009).
22. R. Toda, J. Taniguchi, R. Asano, T. Matsushita, and N. Wada, *J. Low Temp. Phys.* **138**, 177 (2005).
23. The figure shows recent result for 2.4 nm pores.
24. To observe the superfluid shift of an isolated nanotube of the length L, whose third sound velocity is v_3, by a oscillation method with angular velocity ω, ω must be much larger than v_3/L. If $v_3 = 50$ m/s and $L = 300$ nm, 10^3 Hz of the torsional oscillator frequency is much smaller than $v_3 / L \approx 10^{10}$ Hz. Both superfluid shifts of the nanotubes and the films on the grain surfaces are observed only below the 2D KT temperature.
25. Junko Taniguchi, Yosuke Aoki, and Masaru Suzuki, *Phys. Rev. B* **82**, 104509 (2010).
26. J. Taniguchi, K. Demura, and M. Suzuki, *J. Low Temp. Phys.* **171**, 644 (2013).

27. Seiji Miyashita, Hidetoshi Nishimori, Akira Kuroda, and Masuo Suzuki, *Prog. Theor. Phys.* **60**, 1669 (1978).
28. T. Matsubara and H. Matsuda, *Prog. Theor. Phys.* **16**, 569 (1956).
29. Superfluid is a potential flow whose velocity is given as $v_S = (\hbar / m)\nabla\theta$. Increase of the free energy by the flow of the superfluid density σ_S is described as $\Delta f = (1/2)\sigma_S v_S^2$, where v_S is proportional to a phase difference $\Delta\theta$. In the case of the XY spin lattice, the increase of the free energy due to the phase difference $\Delta\theta$ between two sides is described as $\Delta f = (1/2)\Upsilon(\Delta\theta)^2$, where Υ is called as the helicity modulus. Υ in the XY spin system is assumed to correspond to σ_S of the superfluid.
30. K. Yamashita and D.S. Hirashima, private communications.
31. S.I. Shevchenko, *Fiz. Nizk. Temp*. **14**, 1011 (1988) [*Sov. J. Low Temp. Phys*. **14**, 553 (1988)].
32. J. Machta and R.A Guyer, *J. Low Temp. Phys.* **74**, 231 (1989).
33. Nikolai V. Prokof'ev and Boris V. Svistunov, *Phys. Rev. B* **61**, 11282 (2000).
34. Adrian Del Maestro and Ian Affleck, *Phys. Rev. B* **82**, 060515 (2010).
35. M. Tsukamoto and M. Tsubota, *J. Low Temp. Phys.* **162**, 603 (2011).
36. A. Kotani, K. Yamashita, and D.S. Hirashima, *Phys. Rev. B* **83**, 174515 (2011).
37. Thomas Eggel, Miguel A. Cazalilla, and Masaki Oshikawa, *Phys. Rev. Lett.* **107**, 275302 (2011).
38. Ippei Danshita and Anatoli Polkovnikov, *Phys. Rev. A* **85**, 023638 (2012).